ARTICLE

OBC
www.rsc.org/obc

Synthesis and physical properties of biquinoxalinyl bridged bis-porphyrins: models for aspects of Photosynthetic Reaction Centres

Maxwell J. Crossley,* Paul J. Sintic, Robin Walton and Jeffrey R. Reimers
School of Chemistry, The University of Sydney, NSW 2006, Australia.
E-mail: m.crossley@chem.usyd.edu.au

Received 17th April 2003, Accepted 17th June 2003
First published as an Advance Article on the web 7th July 2003

The synthesis of biquinoxalinyl-bridged bis-porphyrin **4** and metallated derivatives **5**–**11** was achieved in high yields. UV-visible spectroscopy and electrochemical experiments indicated weak orbital coupling of the two quinoxalinyl units but minimal orbital coupling between the two porphyrins. The weak electronic communication is attributed to non-planarity, on average, of the molecule because of rotation about the inter-quinoxalinyl connection. This, combined with poor coupling across the fused junctions between the porphyrin and quinoxalinyl units, results in minimal inter-porphyrin communication. As a result, the biquinoxalinyl linkage is appropriate for inclusion in more elaborate synthetic compounds, such as the tris-porphyrin **1**, that are designed to model the charge-separation apparatus of Photosynthetic Reaction Centres.

Introduction

Porphyrin arrays are often used to study electron- and energy-transfer processes due to their great similarity with natural systems. In the Photosynthetic Reaction Centres (PRCs) porphyrinic macrocycles are assembled into arrays where light energy is converted into electrical energy and then chemical energy with high efficiency.[1,2] The structure of the PRCs of purple bacteria[3] and Photosystems I and II of the cyano-bacterium *Synechococcus elongatus*[4,5] show a very similar arrangement of the porphinoid pigments involved in charge separation. In order to mimic this natural process, a number of synthetic systems have been designed in which two or more porphyrins are linked by conjugated bridges through either the *meso*- or β-pyrrolic positions on the porphyrin macrocycle,[6–9] through β-positions by supramolecular assemblies[10–12] or by direct linkage.[13,14] These systems were designed to create an energy gradient to enable the unidirectional transfer of energy or electrons with possible photovoltaic and photonic applications.[15] In addition, most of these systems have been designed with the aim of maximising the electronic communication between the porphyrins.

A target of our work is the covalently linked tris-porphyrin **1** which we propose as a model for the typically *weakly* coupled (bacterio)chlorophyll molecules found in the special pair and primary electron acceptor of the bacterial PRC. This model contains a Tröger's base linkage that establishes C_2 symmetry in the charge separation special pair thereby mimicking an important aspect of the PRC. Also, it contains a biquinoxalinyl linkage. Tris-porphyrin **1** is also an accurate distance model for the PRC with inter-chromophoric distances that closely match the natural system (Table 1).[16] The insertion of metal ions into the terminal chromophores of the tris-porphyrin **1** creates a redox gradient that should facilitate multistep electron-transfer from the zinc(II) porphyrin to the gold(III) porphyrin. Additionally, as both linkages facilitate poor inter-porphyrin conjugation, photoinduced charge separation is expected to be long-lived. On the route to tris-porphyrin **1**, we have developed syntheses of bis-porphyrin systems with each of the required linkers. In a preliminary communication we reported the synthesis of bis-porphyrin **4** and its dizinc(II) derivative **5**.[17] We have also examined the photophysics of the monogold(III) adduct **10**.[18]

The route to these compounds uses the porphyrin-2,3-dione **2** and porphyrin-2,3,12,13-tetraone systems that we developed in other work for the synthesis of laterally-bridged oligo-porphyrins such as the bis-porphyrins and analogous tris-,

Table 1 Distance[16] (Å) between macrocyclic rings of tris-porphyrin **1** (*anti*-planar $\chi = 180°$) compared to the donor–acceptor pair (D–A pair) found in the PRC

Porphyrin units	Edge-to-edge	Centre-to-centre
ZnP–FbP	9.2	16.5
FbP–AuP	10.7	18.7
ZnP–AuP	27.8	34.9
D–A pair	9.5	16.5

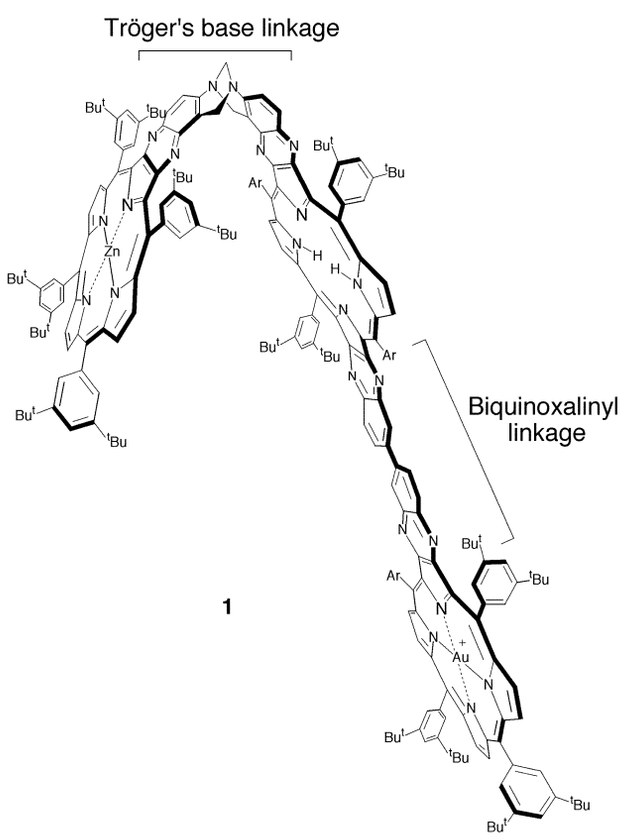

1

DOI: 10.1039/b304161a

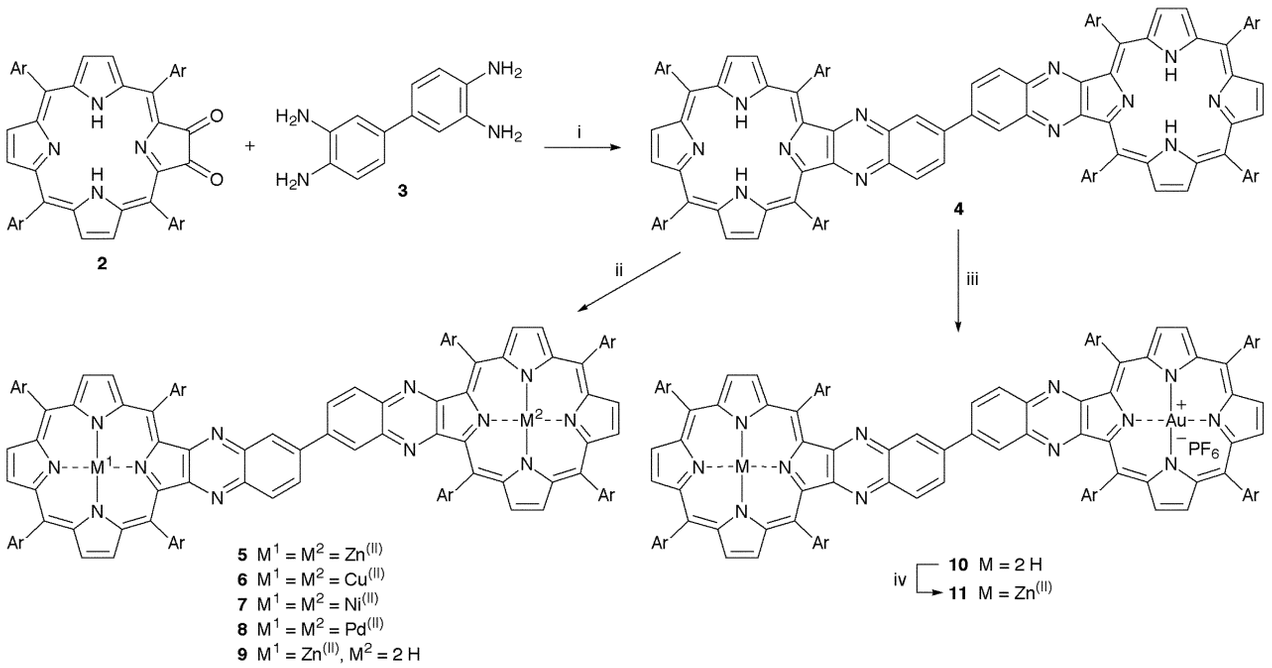

Scheme 1 *Reagents and conditions*: i, CH_2Cl_2, 2 h; ii, metal salt (see text); iii, $KAuCl_4$, NaOAc, AcOH–$CHCl_3$, Δ, then KPF_6 anion exchange; iv, $Zn(OAc)_2{\cdot}2H_2O$, MeOH–$CHCl_3$, Δ, 4 h (Ar = 3,5-$Bu^t_2C_6H_3$).

tetrakis-, pentakis- and hexakis-porphyrins.[19–22] The inter-porphyrin linkages in these compounds were generated by reactions with 1,2,4,5-benzenetetraamine, which establishes a tetraazaanthracene bridge and results in a porphyrin-centre to porphyrin-centre distance of 16.9 Å. Use of 3,3′-diaminobenzidine **3** analogously results in the formation of biquinoxalinyl linked bis-porphyrins (Scheme 1).

In this paper we give full details of the synthesis of the bis-porphyrins **4**–**11**, together with model quinoxalino[2,3-*b*]-porphyrins **13**–**18** and we describe electrochemical, absorption spectroscopy, and electronic-structure modelling studies that assess the suitability of this linker to be used in systems designed to exhibit photo-induced energy- and electron-transfer properties.

Results and discussion

Synthesis

Free-base biquinoxalinyl bis-porphyrin **4** was synthesised by addition of 3,3′-diaminobenzidine **3** to excess 2,3-dioxo-5,10,15,20-tetrakis(3,5-di-*tert*-butylphenyl)chlorin **2** in dichloromethane at room temperature (Scheme 1). A rapid reaction ensued and the product precipitated from solution over 2 hours. Chromatography and crystallisation afforded the bis-porphyrin **4** in 89% yield. Reaction in chloroform gave a similar yield of **4** but without precipitation of the product. When stoichiometric amounts of dione **2** and tetraamine **3** (2 : 1) were employed, the yield of **4** was only 64%. Incompletely cyclised products were never observed. It would seem that the two orthogonal aryl groups flanking the dione unit provide a steric pathway that directs the incoming diamine group so that it always reacts in a double condensation mode.

Spectroscopy confirmed the structure of **4** and ^{1}H NMR revealed the symmetry of the compound. The resonances of the protons on the rings joined by the inter-quinoxalinyl connection displayed the expected AMX splitting pattern for resonances of protons on 1,2,4-trisubstituted benzene rings. The spectrum showed a higher degree of symmetry than that expected for a biquinoxalinyl bridged bis-porphyrin with a non-planar conformation. Low temperature ^{1}H NMR spectra of **4** were acquired at 220 and 230 K and showed no broadening of proton signals providing evidence that the molecule must be rapidly twisting about the inter-quinoxalinyl connection.

Metallated derivatives **5**–**11** were also prepared and physical properties of these molecules were determined to gain a preliminary understanding of the electronic processes occurring in the biquinoxalinyl bis-porphyrin system.

Dizinc(II) biquinoxalinyl bis-porphyrin **5** was obtained in 86% yield by treatment of the free-base bis-porphyrin **4** with zinc(II) acetate dihydrate (Scheme 1). The absence of NH stretches in the infrared spectrum of the dizinc(II) bis-porphyrin **5** indicated that metallation was complete. The zinc(II) bis-porphyrins prepared in this work were all found to demetallate rather easily. Accordingly, chromatography was avoided where possible and when it was used only short plugs of silica were employed. The demetallation of products was particularly facile during chromatography in light.

Dicopper(II) biquinoxalinyl bis-porphyrin **6** was prepared in 77% yield by adding a slurry of copper(II) acetate monohydrate in methanol to a solution of the free-base bis-porphyrin **4** in chloroform and heating the mixture at reflux for 3 hours (Scheme 1). Dinickel(II) bis-porphyrin **7** was prepared by the addition of nickel(II) acetate tetrahydrate in glacial acetic acid to a chloroform solution of bis-porphyrin **4** in 81% yield (Scheme 1). Metallation using *N,N*-dimethylformamide and the metal chloride was not possible as the free-base bis-porphyrin **4** is insoluble in this solvent.

Dipalladium(II) biquinoxalinyl bis-porphyrin **8** was prepared in 98% yield by adding palladium(II) chloride to a solution of free-base bis-porphyrin **4** in toluene and glacial acetic acid and heating the mixture at reflux for 72 hours (Scheme 1).

Monozinc(II) biquinoxalinyl bis-porphyrin **9** was obtained by treatment of **4** with one equivalent of zinc(II) acetate dihydrate (Scheme 1). This reaction resulted in a mixture of the free-base **4**, monozinc(II) **9** and dizinc(II) **5** bis-porphyrins. This mixture was easily separated using flash chromatography and the monozinc(II) product **9** was obtained in 35% yield. Chromatography was performed immediately with protection from light as the unstable metallation product **9** rapidly demetallated.

Zinc(II)-gold(III) bis-porphyrin **11** was prepared by first heating free-base biquinoxalinyl bis-porphyrin **4** in refluxing acetic

acid and chloroform for 72 hours in the presence of potassium tetrachloroaurate(III) and sodium acetate (Scheme 1). The formation of the monogold(III) adduct **10** in a yield above that expected statistically was the result of its partial precipitation during the reaction, coupled with a slow rate of metallation. Anion exchange was then performed on the crude product by stirring in the presence of potassium hexafluorophosphate. The product was purified by flash chromatography to give [monogold(III) bis-porphyrin]PF_6 **10** in a yield of 60%. [Monogold(III) bis-porphyrin]PF_6 **10** was then heated with zinc(II) acetate dihydrate (2 eq.) in chloroform and methanol, followed by basic work up, anion exchange and flash chromatography to give [zinc(II)-gold(III) bis-porphyrin]PF_6 **11** in 87% yield (Scheme 1). The overall yield for the two step reaction was 52%. Microanalysis failed to give meaningful results probably because of the weakly bound nature of the anion, which led to difficulties in recrystallisation of **10** and **11** from chloroform–light petroleum and possible partial counterion exchange. These gold(III) chelated derivatives have applications in photo-induced electron-transfer. The photophysical analysis of **10** has been reported elsewhere,[18] while the zinc(II)-gold(III) bis-porphyrin **11** is still under investigation.[23] The alternative sequence of metallation by way of the monozinc(II) adduct **9** is not appropriate as zinc(II) porphyrins readily demetallate under the conditions required to insert gold(III).

Monomer quinoxalino[2,3-*b*]porphyrins were also synthesised in order to provide comparisons with bis-porphyrins **4**–**11** when determining physical properties. 5,10,15,20-Tetrakis(3,5-di-*tert*-butylphenyl)quinoxalino[2,3-*b*]porphyrin **13** fulfilled this role and was synthesised in 92% yield by stirring a solution of porphyrin-2,3-dione **2** in dichloromethane with *o*-phenylenediamine **12** (5 eq.) at room temperature for 6 hours (Scheme 2). The ^{1}H NMR (400 MHz) spectrum of quinoxalino[2,3-*b*]porphyrin **13** shows the C_{2v} symmetry of the compound. Two multiplets at δ 7.72–7.75 and 7.82–7.85 indicated the four quinoxaline protons. The absence of carbonyl stretches in the infrared spectrum, mass spectroscopy and elemental analysis confirmed the structure of **13**.

The zinc(II), copper(II), nickel(II), palladium(II) and gold(III) chelates **14**–**18** of quinoxalino[2,3-*b*]porphyrin **13** were also prepared in 82, 89, 64, 88, and 51% yields, respectively, using the standard metallation methods to complete the series of comparisons (Scheme 2).

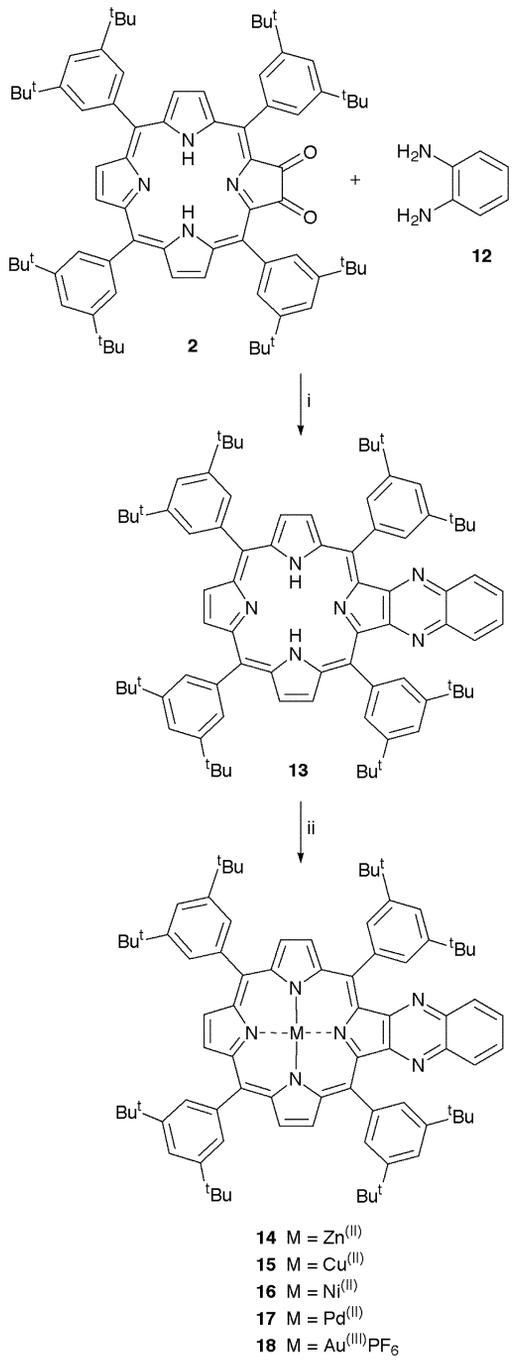

Scheme 2 *Reagents and conditions*: i, CH_2Cl_2, 6 h; ii, see text.

Modelling

The structures of the derivatives of **4** and **13** in which the 3,5-di-*tert*-butylphenyl groups are replaced with hydrogens were determined using the B3LYP density functional calculations[24] with the 3-21G basis set[25] by Gaussian-98.[26] For biquinoxalinyl bis-porphyrin **4**, the calculated dihedral angle about the inter-quinoxalinyl connection is 40°. Electronic couplings were obtained from electron affinities estimated as the unoccupied-orbital eigenvalues and are thus somewhat crude approximations. The vertical excitation energies of **13** were evaluated by our program[27] using INDO/S.[28]

Electrochemical properties

The electronic properties of the biquinoxalinyl bis-porphyrin system were investigated using cyclic voltammetry. Potentials for the quinoxalino-porphyrins (MPQ) **13**–**17** and their corresponding biquinoxalinyl bis-porphyrins [(MPQ-)$_2$] **4**–**8** are provided (Table 2), as are the observed voltammograms for the free-base molecules (Fig. 1). These results are characteristic of those for the other molecules, with the greatest variations found in fact for the nickel(II) species; some specific issues affecting the zinc(II) derivatives are also discussed later. Basically, the voltammograms show only minor variations associated with interconnection of the quinoxalinyl units to form the bis-porphyrins. This is in stark contrast to the behaviour of conjugated bis-porphyrin **19** which has four rather than two distinct reversible one-electron reductions occurring at low voltage. Changes in the voltammograms on dimer formation originate through incompletely screened electrostatic interactions operating between the two halves, and from couplings of the fragment molecular orbitals of each half. The relatively minor changes observed for the biquinoxalinyl bis-porphyrins indicate that the Coulombic screening is nearly complete and the orbital interactions are minor whilst the profound effects observed for **19** indicate significant orbital interactions and inter-porphyrin coupling within this rigid fused molecule.

The differences between the cyclic voltammograms of the quinoxalino-porphyrins and the biquinoxalinyl bis-porphyrins largely comprise small changes in the potentials and significant peak broadening. These provide information concerning the specific chemistry of the species and some indication of residual inter-orbital interactions. In order to understand these effects, pictures of the orbitals of a free-base mono-porphyrin are

Table 2 Summary of redox potentials (in V) obtained for free-base and dimetallated biquinoxalinyl bis-porphyrins **4**–**8** and free-base and metallated quinoxalino-porphyrins **13**–**17**. All measurements were obtained in THF, scan rate 100 mV s^{-1}, referenced to Ag/AgCl and containing 0.1 M TBAP

		Macrocycle reduction ($E_{1/2}$)		Bridge reduction (E_p)			Oxidation ($E_{1/2}$)		
Compound		R_1	R_2	R_3	R_4	R_5	Ox_1	Ox_2	Δ (1st Ox − 1st Red)
4	$(2HPQ\text{-})_2$	−1.02	−1.21	−2.24	−2.64	−2.79	1.28[a]		2.30
13	2HPQ	−1.03	−1.25	−2.24	−2.64	−2.80	1.26[a]		2.29
5	$(ZnPQ\text{-})_2$	−1.18	−1.81[a]	−2.40[b]	−2.80		1.04	1.22	2.22
14	ZnPQ	−1.18	−1.55	−2.27	−2.95		1.02	1.13	2.20
6	$(CuPQ\text{-})_2$	−1.03	−1.44	−2.26	−2.76		1.21		2.24
15	CuPQ	−1.07	−1.46	−2.15	−2.77		1.20		2.27
7	$(NiPQ\text{-})_2$	−1.07[a]	−1.44	−2.36	−2.72		1.12		2.19
16	NiPQ	−1.04	−1.46	−2.25	−2.66		1.10		2.14
8	$(PdPQ\text{-})_2$	−1.04	−1.46	−2.32	−2.78		1.37		2.41
17	PdPQ	−1.04	−1.45	−2.14	−2.76		1.38		2.42

[a] E_p value. [b] Peak distorted due to absorption.

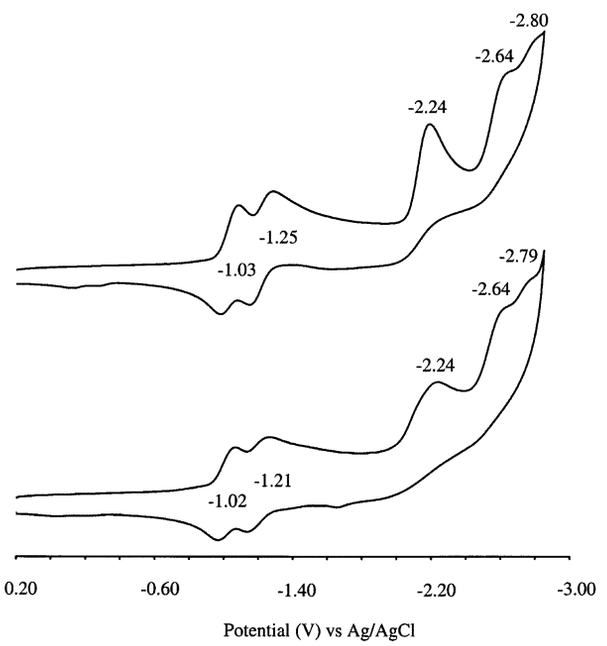

Fig. 1 Cyclic voltammograms obtained upon the reduction of free-base quinoxalino[2,3-*b*]porphyrin **13** (top) and free-base biquinoxalinyl bis-porphyrin **4** (bottom) in THF containing 0.1 M TBAP.

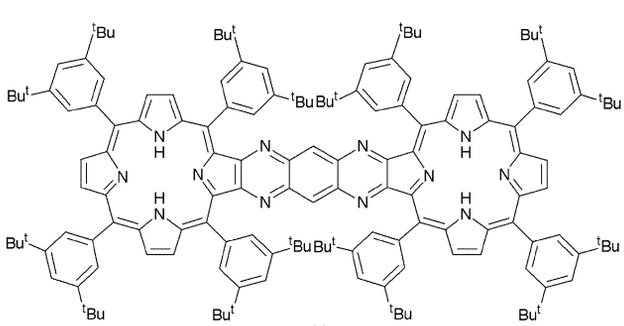

19

provided (Fig. 2) as obtained from density-functional calculations. This shows the lowest-unoccupied molecular orbital and the following four orbitals, named L_1 to L_5, respectively. Most importantly, the orbitals can be partitioned into those that are largely localised on the porphyrin (L_1 and L_2), those localised on the appended quinoxaline (L_3 and L_5), and one largely porphyrin orbital with some quinoxaline delocalisation (L_4). The orbital L_4 is known not to contribute to the electrochemistry of porphyrins and to make only a minor contribution to their spectroscopy and is discussed no further. In biquinoxalinyl bis-porphyrins, coupling between the monomeric units

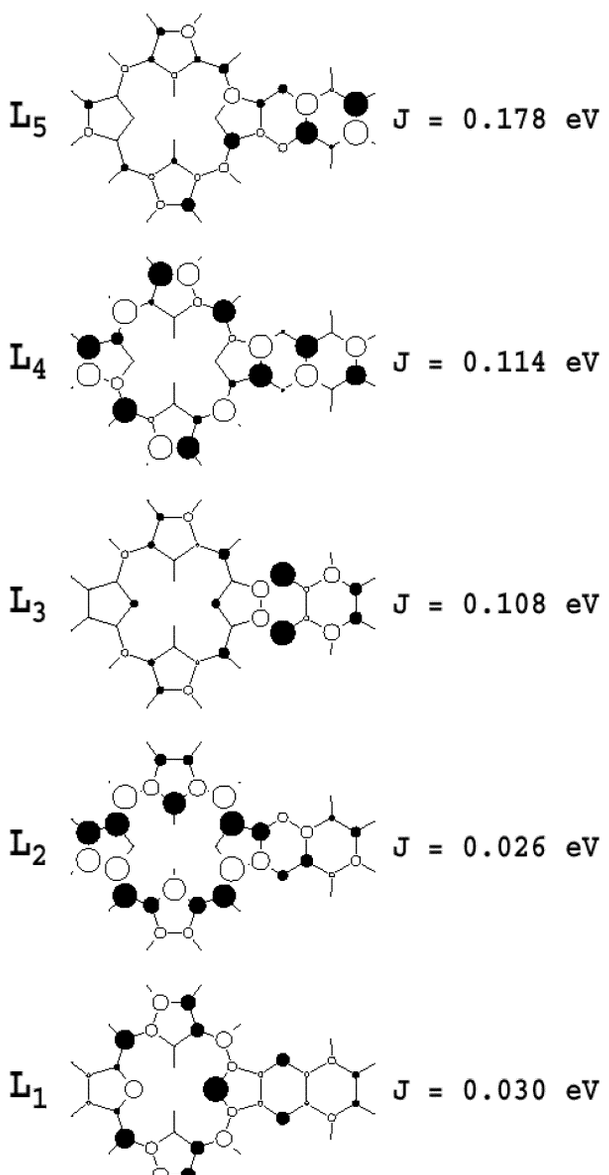

Fig. 2 The nature of the five lowest-energy unoccupied orbitals from B3LYP calculations of **13** and the coupling *J* between matching orbitals (L_n–L_n) in the biquinoxalinyl bis-porphyrin **4**.

is related to the orbital coefficient on the atoms that form the inter-quinoxalinyl connection; quantitatively, the values of the orbital couplings *J* obtained from density-functional

Table 3 Summary of redox potentials (in V) obtained for bis-porphyrin **9** and quinoxalino-porphyrins **13** and **14**. Measurements were obtained in THF, scan rate 100 mV s^{-1}, referenced to Ag/AgCl and containing 0.1 M TBAP

Compound	Macrocycle reduction ($E_{1/2}$)			Bridge reduction (E_p)		Oxidation ($E_{1/2}$)	
9	−1.00	−1.17[a]	−1.75	−2.33[a]	−2.73	1.06	1.32[a,b]
13	−1.03	−1.25		−2.24	−2.64		1.26[b]
14		−1.18	−1.81[b]	−2.27	−2.95	1.02	1.13

[a] Broad peaks, indicating a superposition of redox process on both the ZnP and FbP in **9**. [b] E_p value.

calculations on the corresponding free-base bis-porphyrin are also provided (Fig. 2).

Reductions R_1 and R_2 (Table 2) are reversible one-electron processes that have been assigned to the porphyrin sub units.[29] Isolated porphyrins display similar reductions associated with just one orbital, identified as L_1 by the density-functional calculations (Fig. 2). Similar reductions involving orbital L_2 are not expected within the accessible voltage range, and the reductions R_3 and R_4 have been attributed to the quinoxaline subunits.[29] From the calculations, these processes are assigned to orbital L_3. The degree of broadening of R_3 observed for the bis-porphyrins is greater than that observed for R_1 and R_2, as anticipated by the calculated increase in coupling J from 0.030 to 0.114 eV (Fig. 2); intuitively, R_3 is expected to separate into two resolvable components if the coupling is as high as the value of 0.114 eV predicted for R_4, however, supporting the orbital assignment. The free-base species **4** and **13** (Fig. 1) also display a resolved fifth reduction named R_5 at −2.80 V, just before the onset of solvent reduction.

Strong adsorption of dizinc(II) biquinoxalinyl bis-porphyrin **5** to the electrode, impaired analysis of this system by electrochemical studies. It cannot be determined whether the first quinoxaline bridge reduction is split or if the cyclic voltammogram is distorted by deposition (Table 2). In contrast, the cyclic voltammogram of monozinc(II) biquinoxalinyl bis-porphyrin **9** revealed that each chromophore has equivalent electrochemical behaviour to the corresponding free-base and zinc(II) quinoxalino[2,3-*b*]porphyrins **13** and **14** (Table 3). Thus, the asymmetric system **9** is weakly coupled displaying similar trends to those observed for the free-base, dicopper(II) and dipalladium(II) biquinoxalinyl bis-porphyrin chelates **4**, **6**, and **8**.

Substantial differences were observed when dinickel(II) biquinoxalinyl bis-porphyrin **7** was compared to nickel(II) quinoxalino[2,3-*b*]porphyrin **16** (Fig. 3 and Table 2). Cycles of the first reduction, of the first two reductions and of the first three reductions revealed that the first macrocyclic reduction in the bis-porphyrin **7** is irreversible but the second macrocyclic reduction ($E_{1/2}$ = 1.44 V) is reversible and approximately equal to that of the model quinoxalino[2,3-*b*]porphyrin **16**. The quinoxaline reductions in the bis-porphyrin **7** occurred at more negative potentials than the reductions of **16** and the current increased. The origin of the enhancement is yet to be determined but it might be due to distortions of the porphyrin macrocycle affecting the overall structure. Such distortions are a common feature of nickel(II) porphyrins and a phenomenon used to explain anomalous results in other electrochemical studies.[30,31]

Oxidation processes were also examined for the free-base and metal(II) biquinoxalinyl bis-porphyrins (Tables 2 and 3). The dimetallated adducts gave a single well defined 'quasi-reversible' oxidation, with the exception of the dizinc(II) analogue **5** which gave two reversible one-electron oxidative processes. Likewise, the metallated quinoxalino[2,3-*b*]-porphyrins showed an identical trend to their corresponding bis-porphyrin analogues. Multistep electron-transfer processes occur in copper(II), nickel(II) and palladium(II) bis-porphyrins **6**–**8** as the peak current intensity is approximately twice the size of the corresponding first reduction. The presence of the free-base macrocycle in bis-porphyrin **4** and monozinc(II) bis-porphyrin **9** resulted in irreversible oxidative processes. In

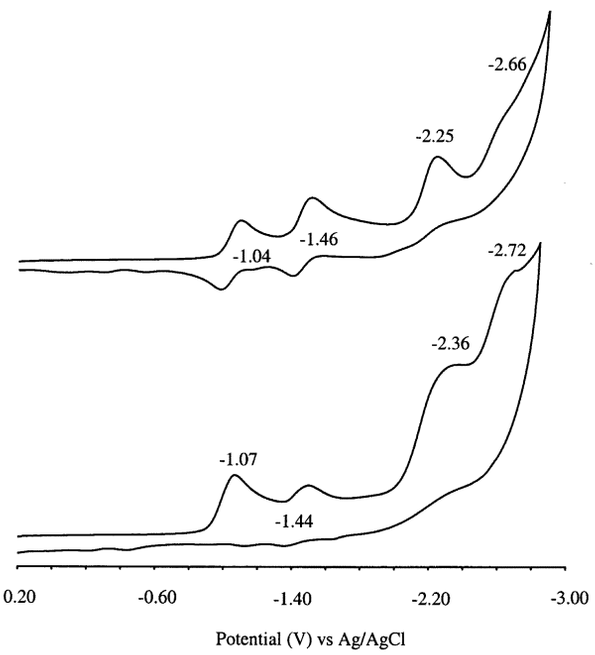

Fig. 3 Cyclic voltammograms obtained upon the reduction of nickel(II) quinoxalino[2,3-*b*]porphyrin **16** (top) and dinickel(II) biquinoxalinyl bis-porphyrin **7** (bottom) in THF containing 0.1 M TBAP.

all the above biquinoxalinyl bis-porphyrins, oxidation potentials were almost identical to respective monomeric components, again indicative of weak coupling. The separation between the first oxidation and the first reduction, the HOMO-LUMO gap, for all the derivatives **4**–**8** fell within the expected range of 2.25 ± 0.20 V.

We have previously reported the photophysical properties of monogold(III) biquinoxalinyl bis-porphyrin **10**.[18] Electrochemical investigation of this metal(III) system when compared to its constituent monomeric components, free-base and gold(III) quinoxalino[2,3-*b*]porphyrins **13** and **18** (Fig. 4), revealed that the system is weakly coupled. The bis-porphyrin **10** undergoes eight one-electron reductions that can be assigned to the free-base macrocycle (FbP), the gold(III) macrocycle (AuP) and biquinoxalinyl bridge components. The first redox process is assigned to the AuP and is a metal-centred Au^{III}/Au^{II} reduction.[32] The following macrocycle-centred reductions in **10** were similar to the model compounds (indicating weak communication) with the exception of the sixth and seventh reductions at E_p = −2.14 and −2.38 V, which are tentatively assigned to the first quinoxaline reductions of the FbP and AuP macrocycles in **10**. These peak potentials appear to have been split by 240 mV when compared to the molecular components, components that are reduced at virtually the same potential as each other. This could be an indication of significantly enhanced interaction across the inter-quinoxalinyl connection. Alternatively, we note that the corresponding digold(III) molecule could not be readily isolated as it underwent decomposition of the linkage, and the triply reduced gold–free base compound may likewise be chemically reactive. Oxidation redox processes in **10** were poorly resolved and no useful information could be obtained.

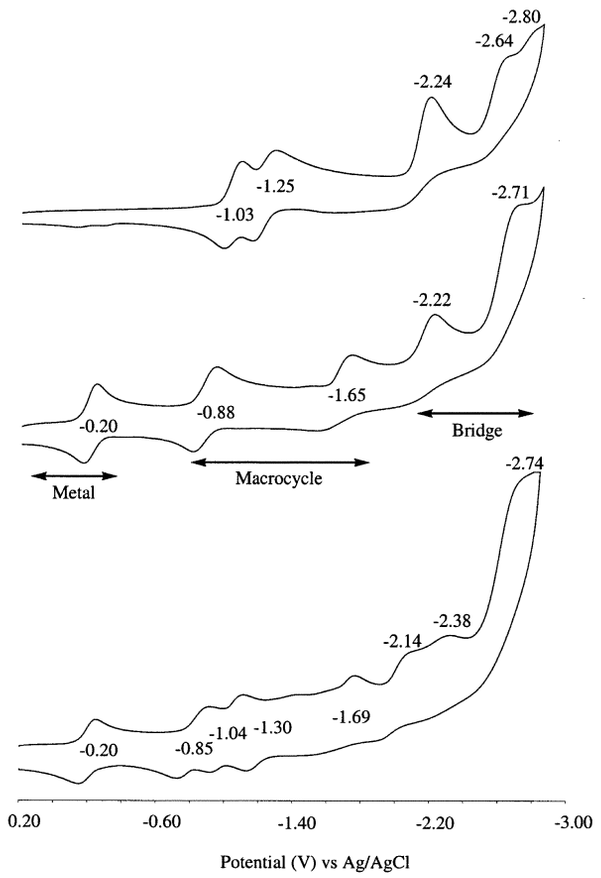

Fig. 4 Cyclic voltammograms obtained upon the reduction of free-base quinoxalino[2,3-*b*]porphyrin **13** (top), gold(III) quinoxalino[2,3-*b*]-porphyrin **18** (middle) and monogold(III) biquinoxalinyl bis-porphyrin **10** (bottom) in THF containing 0.1 M TBAP.

Comprehensive electrochemical analysis of the quinoxalino[2,3-*b*]porphyrins **13**–**18**, and the biquinoxalinyl bis-porphyrin systems **5**–**11**, in different solvents and other varied conditions is currently in progress.[33]

Absorption spectroscopy

Comparison of UV-visible absorption spectra of model bis-porphyrin systems with those of their monomeric species provides evidence of intramolecular interaction. If there were no intramolecular interactions, the absorption spectrum would be the sum of the monomer spectra. Changes in spectral features, such as splitting, broadening and shifting are indicative of intramolecular interactions.[7] Whole magnitudes of any observed splittings are proportional to the degree of coupling within the molecule[34] but such splittings are often difficult to observe. The observed spectra for the free-base, copper(II), nickel(II), and zinc(II) monomeric and dimeric quinoxalinyl porphyrins (Fig. 5) in deacidified chloroform show, in some cases, signs of significant interactions but in no case can individual band splittings be resolved and hence quantitative analysis provided.

The spectrum of the free-base biquinoxalinyl bis-porphyrin **4** has the same shape as its monomeric component, free-base quinoxalino[2,3-*b*]porphyrin **13**, with slight broadening and a red-shift for the Soret band maxima of 10 nm (Fig. 5a). Little evidence is seen for inter-chromophoric coupling.

Analysis of the Soret-band spectra is somewhat complicated as in all porphyrins this band has two distinct components that may or may not be individually resolvable. In the quinoxalinyl porphyrin monomers, these two components are polarised in the π plane, one in the direction of the bridge, with the other perpendicular. In bis-porphyrins, inter-porphyrin coupling is manifest through splittings of the energies of the analogously polarized Soret components. For the zinc(II) mono-porphyrin **14**, the two components of the Soret band are individually identifiable, with one of these moving to significantly lower energy compared to the free-base analogue. This feature is retained in the spectrum of the dizinc(II) species **5**. However, a shoulder in the spectrum of both molecules is apparent at *ca.* 470 nm, and it is clear that the lower-energy Soret component loses significantly more intensity to this shoulder in the bis-porphyrin than it does in the monomer. Hence it is clear that this 470 nm shoulder is affected by some inter-chromophore coupling process. INDO/S calculations predict that the 470 nm shoulder arises from a porphyrin to quinoxaline transition involving the bridge orbital L_5 (Fig. 2). A similar transition is also observed in the spectrum of the significantly coupled bis-porphyrin **19**, and both INDO/S as well as *ab initio* CIS, RPA, and CASPT2 calculations[35] interpret it analogously. The observed spectral shape changes on dimerisation are thus attributed to intermediate-strength coupling acting between the two quinoxalines in the biquinoxalinyl species. No indication of inter-porphyrin coupling is evident, however. For the copper(II) and nickel(II) porphyrins (Fig. 5), the metal induces larger red shifts of the lower-energy Soret component than those found for zinc(II) porphyrins. This enhances its interaction with the 470 nm porphyrin to quinoxaline transition, making the latter more pronounced. For the dinickel(II) bis-porphyrin **7**, the lower Soret and porphyrin to quinoxaline transitions are of equal intensity and individually resolved at 464 and 472 nm, respectively.

Conclusions

An efficient synthesis of biquinoxalinyl bridged bis-porphyrins has been developed. Through spectroscopic, electrochemical, and modelling studies we have shown that the porphyrin macrocycles contained in biquinoxalinyl bis-porphyrin **4** and all described metallated derivatives are all weakly coupled to each other.

The minimal coupling between porphyrin rings in this system can be attributed to the nature of the inter-quinoxalinyl linkage and to the degree of mixing between the porphyrin and quinoxaline orbitals. The electronic absorption spectra indicate that transitions of a porphyrin to quinoxaline nature in monomeric species are significantly perturbed in the spectra of the corresponding biquinoxalinyl bis-porphyrins. This is interpreted as arising from coupling of the quinoxaline based orbitals L_5 (Fig. 2) across the inter-biquinoxalinyl connection. The corresponding cyclic voltammograms show even less perturbations in going from quinoxalino-porphyrins to biquinoxalinyl bis-porphyrins, even for reduction processes involving quinoxaline orbitals. This is interpreted as arising from the involvement of a different, much less coupled bridge orbital, L_3. The weak inter-porphyrin couplings observed in the systems studied indicate that these compounds provide essential key features required in model systems for the operation of PRCs.

Future work will involve functionalising the biquinoxalinyl bis-porphyrin into larger multiporphyrin arrays. Recently, we have successfully synthesised zinc(II)-free-base-gold(III) tris-porphyrin array **1**, in which the biphenyl linker has been functionalised to extended Tröger's base bis-porphyrin, to act as an accurate distance model of the PRC. It is encouraging that a molecular component of tris-porphyrin **1**, monogold(III) biquinoxalinyl bis-porphyrin **10**, exhibits weak ground-state interaction and rapid electron-transfer.[18] The synthesis and photophysical properties of **1** will be reported elsewhere.

Experimental

General procedures

Melting points were recorded on a Riechert melting point stage and are uncorrected. Microanalyses were performed by the

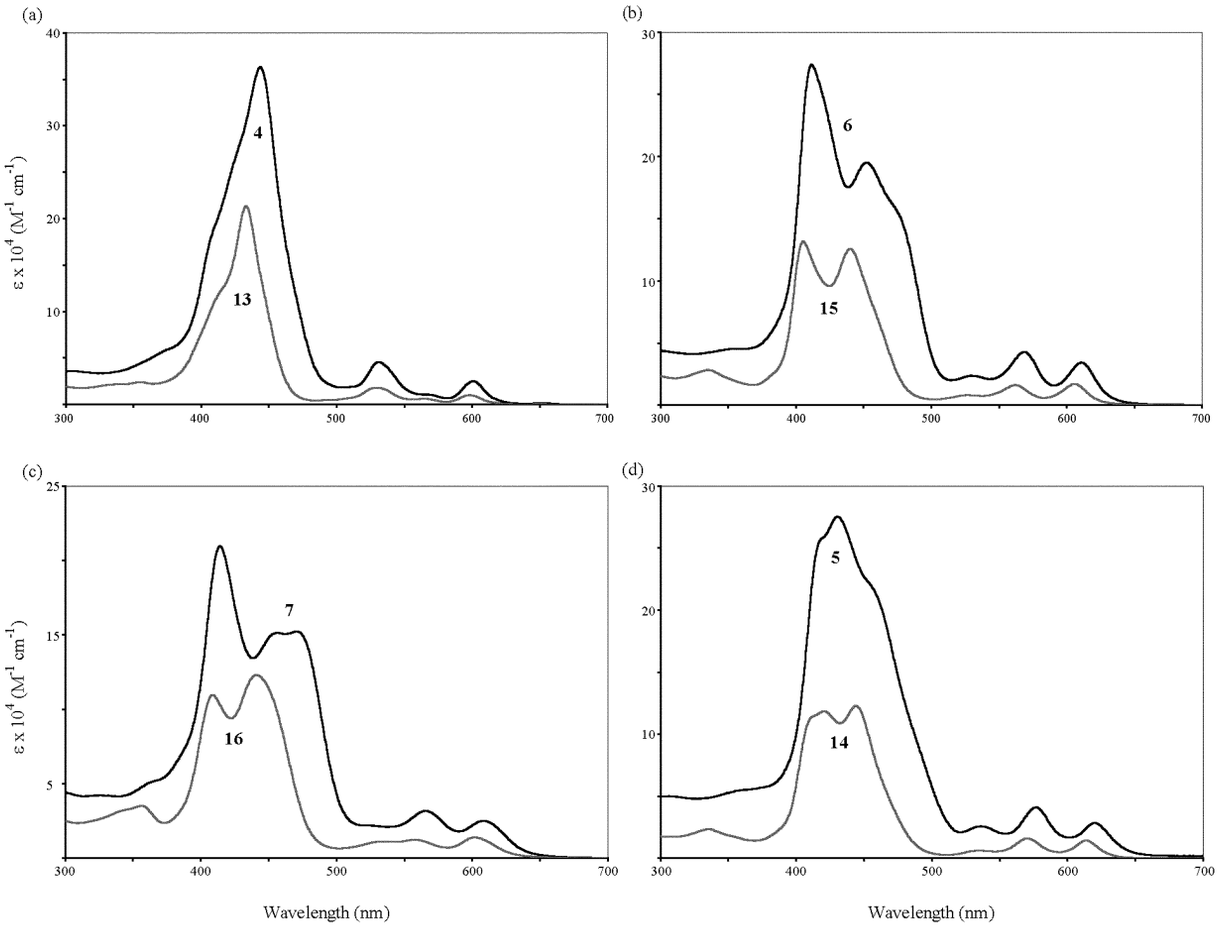

Fig. 5 UV-visible absorption spectra ($CHCl_3$) of: (a) free-base biquinoxalinyl bis-porphyrin **4** and free-base quinoxalino[2,3-*b*]porphyrin **13**, (b) dicopper(II) biquinoxalinyl bis-porphyrin **6** and copper(II) quinoxalino[2,3-*b*]porphyrin **15**, (c) dinickel(II) biquinoxalinyl bis-porphyrin **7** and nickel(II) quinoxalino[2,3-*b*]porphyrin **16**, (d) dizinc(II) biquinoxalinyl bis-porphyrin **5** and zinc(II) quinoxalino[2,3-*b*]porphyrin **14**.

Australian Microanalytical Service, National Analytical Laboratories, Ferntree Gully, Victoria, or the Microanalytical Unit, The University of New South Wales, Australia.

Infrared spectra were determined on a Digilab FTS 20/80 or on a Perkin-Elmer Model 1600 FT-IR spectrophotometer as solutions in the stated solvents. Unless otherwise stated, electronic spectra were determined as chloroform solutions with an Hitachi 150–20 or Cary 5E UV-Vis-NIR spectrophotometer. ^{1}H NMR spectra were recorded on a Bruker WM-400 (400 MHz) or AMX-400 (400 MHz) spectrometer, with tetramethylsilane (Me_4Si) as the internal standard. Signals are recorded in terms of chemical shift (δ) in ppm from Me_4Si, multiplicity, coupling constants (in Hz) and assignments, in that order. ^{31}P NMR spectra were acquired on a Bruker DPX-400 (162 MHz) spectrometer. ^{31}P NMR chemical shifts are referenced to external, neat trimethyl phosphite taken to be 140.85 ppm at room temperature. The following abbreviations for multiplicity are used: s, singlet; d, doublet; t, triplet; m, multiplet; h, heptet; dd, doublet of doublets; ABq, AB quartet.

Matrix assisted laser desorption ionisation time of flight (MALDI-TOF) mass spectra without a matrix were recorded on a VG TofSpec spectrometer. Electron impact (EI) ionisation mass spectra were recorded on a Kratos MS902 mass spectrometer which was connected to a Kratos DS 90 data handling system. Fast atom bombardment high resolution mass spectra (FAB-HRMS) were recorded on a VG ZAB-2SEQ instrument at the Research School of Chemistry, Australian National University.

Column chromatography was routinely carried out using flash chromatography on Merck silica gel Type 9385 (230–400 mesh). Analytical thin layer chromatography (TLC) was performed on Merck silica gel 60 F_{254} precoated sheets (0.2 mm). All solvents used for chromatography were redistilled before use, unless otherwise stated. Light petroleum refers to the fraction of bp 60–80 °C. Where solvent mixtures were used, the proportions are given by volume. All solvents used for recrystallisations were redistilled before use, unless otherwise stated.

Electrochemistry was performed using a BAS 100 Electrochemical Analyzer. All measurements were made at room temperature, unless otherwise stated, on a sample dissolved in freshly distilled tetrahydrofuran, with 0.1 M tetrabutylammonium perchlorate (TBAP) as the supporting electrolyte. A glassy carbon working electrode, platinum wire auxiliary electrode and an Ag–AgCl–KCl (sat) reference electrode were used. The solutions were de-oxygenated by saturation with oxygen-free argon. The tetrahydrofuran was purified in three steps; first it was dried over sodium wire; and then over sodium wire and benzophenone under nitrogen, and finally freshly distilled over lithium aluminium hydride under nitrogen. The electrolyte was purified by recrystallisation from an ethyl acetate–ether mixture, air dried, and then stored under vacuum over P_2O_5.

Synthesis of biquinoxalinyl bridged bis-porphyrins

6″,6‴-{5,5′,10,10′,15,15′,20,20′-Octakis(3,5-di-*tert*-butylphenyl)quinoxalino[2,3-*b*:2′,3′-*b*′]bisporphyrin} 4. 2,3-Dioxo-5,10,15,20-tetrakis(3,5-di-*tert*-butylphenyl)chlorin **2** (174 mg, 0.159 mmol, 3 eq.) and 3,3′-diaminobenzidine **3** (11.5 mg, 0.054 mmol, 1 eq.) were dissolved in dichloromethane (10 cm^3) and stirred for 2 h. The reaction was followed by TLC (dichloromethane–light petroleum, 1 : 1) until no further reaction was observed to have taken place, and the solvent was removed. The residue was purified by flash chromatography (SiO_2, chloro-

form–light petroleum, 1 : 1). The front-running, tan major fraction was collected and evaporated to dryness. This fraction was recrystallised to yield brown microcrystals of *6″,6‴-{5,5′,10,10′,15,15′,20,20′-octakis(3,5-di-tert-butylphenyl)quinoxalino-[2,3-b:2′,3′-b′]bisporphyrin}* **4** (112 mg, 89%), mp > 300 °C (from dichloromethane and light petroleum). The reaction was repeated using a 2 : 1 ratio of diketone–tetraamine but the yield was only 80.6 mg (64%) (Found: C, 84.6; H, 8.5; N, 7.4. $C_{164}H_{190}N_{12}$ requires C, 84.6; H, 8.2; N, 7.2%); $\nu_{max}(CHCl_3)$/cm^{-1} 3351, 2966, 2906, 2670, 1593, 1478, 1364, 1249 and 922; $\lambda_{max}(CHCl_3)$/nm 303 (log ε 4.66), 373sh (4.79), 407sh (5.25), 423sh (5.46), 444 (5.56), 511sh (4.28), 532 (4.64), 570 (4.03), 601 (4.38), 653 (3.29) and 738 (2.09); δ_H(400 MHz; $CDCl_3$; Me_4Si) −2.47 (4 H, s, inner NH), 1.51–1.60 (144 H, m, *t*-butyl H), 7.85 (2 H, t, *J* 1.8, aryl H), 7.86 (2 H, t, *J* 1.8, aryl H), 8.03 (2 H, d, $J_{8″,7″}$ 9.0, biquinoxalinyl H-8), 8.04–8.07 (8 H, m, aryl H), 8.08 (4 H, d, *J* 1.8, aryl H), 8.12 (4 H, d, *J* 1.8, aryl H), 8.13 (4 H, d, *J* 1.8, aryl H), 8.17 (2 H, dd, $J_{7″,8″}$ 9.0, $J_{7″,5″}$ 2.0, biquinoxalinyl H-7), 8.21 (2 H, d, $J_{5″,7″}$ 2.0, biquinoxalinyl H-5), 8.79 (4 H, s, H-12 and H-13), 9.01 and 9.10 (4 H, ABq, J_{AB} 5.0, β-pyrrolic H), 9.02 and 9.11 (4 H, ABq, J_{AB} 5.0, β-pyrrolic H); *m/z* (MALDI-TOF) 2329 (M^+ requires 2329). Evaporation of the second brown fraction afforded the starting material 2,3-dioxo-5,10,15,20-tetrakis(3,5-di-*tert*-butylphenyl)chlorin **2** (45 mg).

6″,6‴-{5,5′,10,10′,15,15′,20,20′-Octakis(3,5-di-*tert*-butylphenyl)quinoxalino[2,3-*b*:2′,3′-*b*′]bisporphyrinato}dizinc(II) 5. 6″,6‴-{5,5′,10,10′,15,15′,20,20′-Octakis(3,5-di-*tert*-butylphenyl)-quinoxalino[2,3-*b*:2′,3′-*b*′]bisporphyrin} **4** (88 mg, 0.038 mmol) was dissolved in chloroform (7 cm^3). A solution of zinc(II) acetate dihydrate (191 mg, 0.87 mmol) in methanol (4 cm^3) was added and the solution heated at reflux for 4 h. The solvent was removed and the residue was dissolved in chloroform (20 cm^3), washed with water (2 × 20 cm^3), dried over anhydrous sodium sulfate, filtered and the solvent removed. The residue was recrystallised as quickly as possible, minimising exposure to light. The dark brown microcrystals of *6″,6‴-{5,5′,10,10′,15,15′,20,20′-octakis(3,5-di-tert-butylphenyl)quinoxalino[2,3-b:2′,3′-b′]bisporphyrinato}dizinc(II)* **5** were collected (80 mg, 86%), mp > 300 °C (from dichloromethane and methanol). An analytically pure sample of dizinc(II) bis-porphyrin **5** was obtained by passing the compound through a short plug of silica, minimising exposure to light (Found: C, 77.1; H, 7.9; N, 6.6. $C_{164}H_{186}N_{12}Zn_2$ + 1.5 CH_2Cl_2 requires C, 77.1; H, 7.4; N, 6.5%); $\nu_{max}(CHCl_3)$/cm^{-1} 2966, 2906, 2869, 1593, 1478, 1463, 1394, 1364, 1346, 1297, 1248, 1155, 1002 and 938; $\lambda_{max}(CHCl_3)$/nm 360 (log ε 4.69), 419sh (5.41), 432 (5.44), 457sh (5.34), 540 (4.32), 579 (4.61) and 624 (4.46); δ_H(400 MHz; $CDCl_3$; Me_4Si) 1.48–1.58 (144 H, m, *t*-butyl H), 7.81 (2 H, t, *J* 1.9, aryl H), 7.82 (2 H, t, *J* 1.9, aryl H), 7.99 (2 H, t, *J* 1.9, aryl H), 8.02 (4 H, d, *J* 1.9, aryl H), 8.02–8.05 (2 H, m, aryl H), 8.05 (4 H, d, *J* 1.9, aryl H), 8.09 (2 H, d, *J* 9.0, biquinoxalinyl H-8), 8.11 (4 H, d, *J* 1.9, aryl H), 8.12 (4 H, d, *J* 1.9, aryl H), 8.22 (2 H, dd, $J_{7″,8″}$ 9.0, $J_{7″,5″}$ 2.0, biquinoxalinyl H-7), 8.25 (2 H, d, *J* 2.0, biquinoxalinyl H-5), 8.92 (4 H, s, H-12 and H-13), 9.02 and 9.08 (4 H, ABq, J_{AB} 5.0, β-pyrrolic H), 9.03 and 9.09 (4 H, ABq, J_{AB} 5.0, β-pyrrolic H); *m/z* (MALDI-TOF) 2455 (M^+ requires 2456).

6″,6‴-{5,5′,10,10′,15,15′,20,20′-Octakis(3,5-di-*tert*-butylphenyl)quinoxalino[2,3-*b*:2′,3′-*b*′]bisporphyrinato}dicopper(II) 6. A slurry of cupric(II) acetate monohydrate (20 mg, 0.098 mmol) in methanol (4 cm^3) was added to 6″,6‴-{5,5′,10,10′,15,15′,20,20′-octakis(3,5-di-*tert*-butylphenyl)quinoxalino[2,3-*b*:2′,3′-*b*′]-bisporphyrin} **4** (99 mg, 0.043 mmol) in chloroform (30 cm^3) and heated at reflux for 3 h. The reaction mixture was checked by TLC (chloroform–light petroleum, 1 : 1) and found to be complete, thus the solvent was removed. The residue was dissolved in chloroform (40 cm^3) and washed with water (2 × 50 cm^3), dried over anhydrous sodium sulfate, filtered and the solvent removed completely. The compound was purified by flash chromatography (SiO_2, carbon tetrachloride–light petroleum, 1 : 1). The major dark brown band was collected, evaporated to dryness and the residue was recrystallised to give *6″,6‴-{5,5′,10,10′,15,15′,20,20′-octakis(3,5-di-tert-butylphenyl)quinoxalino[2,3-b:2′,3′-b′]bisporphyrinato}dicopper(II)* **6** (80 mg, 77%) as brown microcrystals, mp > 300 °C (from chloroform and light petroleum) (Found: C, 79.5; H, 7.8; N, 6.7. $C_{164}H_{186}N_{12}Cu_2$ + 0.25 $CHCl_3$ requires C, 79.5; H, 7.6; N, 6.8%); $\nu_{max}(CHCl_3)$/cm^{-1} 2966, 2934, 2906, 2871, 1594, 1478, 1467, 1394, 1364, 1351, 1298, 1248, 1159, 1010, 944 and 938; $\lambda_{max}(CHCl_3)$/nm 412 (log ε 5.44), 453 (5.29), 478sh (5.16), 531 (4.37), 569 (4.61) and 611 (4.53); *m/z* (MALDI-TOF) 2453 (M^+ requires 2453).

6″,6‴-{5,5′,10,10′,15,15′,20,20′-Octakis(3,5-di-*tert*-butylphenyl)quinoxalino[2,3-*b*:2′,3′-*b*′]bisporphyrinato}dinickel(II) 7. 6″,6‴-{5,5′,10,10′,15,15′,20,20′-Octakis(3,5-di-*tert*-butylphenyl)-quinoxalino[2,3-*b*:2′,3′-*b*′]bisporphyrin} **4** (155 mg, 0.066 mmol) was dissolved in chloroform (50 cm^3) and a solution of nickel(II) acetate tetrahydrate (80 mg, 0.68 mmol) in glacial acetic acid (30 cm^3) was added. The solution was heated at reflux for 4 h. The organic layer was washed with water (2 × 100 cm^3), and the water extracted with chloroform (30 cm^3). The combined organic extracts were dried over anhydrous sodium sulfate and filtered. The solvent was removed and the residue was purified by flash chromatography (SiO_2, carbon tetrachloride–light petroleum, 1 : 1). The major dark brown fraction was collected, evaporated to dryness and the residue was recrystallised. *6″,6‴-{5,5′,10,10′,15,15′,20,20′-Octakis(3,5-di-tert-butylphenyl)quinoxalino[2,3-b:2′,3′-b′]bisporphyrinato}dinickel(II)* **7** was obtained as dark brown microcrystals (131 mg, 81%), mp > 300 °C (from chloroform and light petroleum) (Found: C, 78.7; H, 7.9; N, 6.7. $C_{164}H_{186}N_{12}Ni_2$ + 0.5 $CHCl_3$ requires C, 79.0; H, 7.5; N, 6.7%); $\nu_{max}(CHCl_3)$/cm^{-1} 2967, 2906, 2869, 1594, 1470, 1465, 1395, 1365, 1355, 1299, 1248, 1159, 1013 and 940; $\lambda_{max}(CHCl_3)$/nm 363sh (log ε 4.53), 415 (5.32), 456 (5.18), 471 (5.18), 524 (4.32), 566 (4.48) and 609 (4.38); δ_H(400 MHz; $CDCl_3$; Me_4Si) 1.44–1.55 (144 H, m, *t*-butyl H), 7.70 (2 H, t, *J* 2, aryl H), 7.71 (2 H, t, *J* 2, aryl H), 7.74 (4 H, d, *J* 2, aryl H), 7.75 (4 H, d, *J* 2, aryl H), 7.82 (2 H, t, *J* 2, aryl H), 7.84 (4 H, d, *J* 2, aryl H), 7.85 (4 H, d, *J* 2, aryl H), 7.87 (2 H, t, *J* 2, aryl H), 7.95 (2 H, d, $J_{8″,7″}$ 9.0, biquinoxalinyl H-8), 8.09 (2 H, dd, $J_{7″,8″}$ 9.0, $J_{7″,5″}$ 2.0, biquinoxalinyl H-7), 8.18 (2 H, d, $J_{5″,7″}$ 2.0, biquinoxalinyl H-5), 8.69 (4 H, s, H-17, H-18, H-17′ and H-18′), 8.76 and 8.86 (4 H, ABq, J_{AB} 5, β-pyrrolic H), 8.77 and 8.88 (4 H, ABq, J_{AB} 5, β-pyrrolic H); *m/z* (MALDI-TOF) 2444 (M^+ requires 2443).

6″,6‴-{5,5′,10,10′,15,15′,20,20′-Octakis(3,5-di-*tert*-butylphenyl)quinoxalino[2,3-*b*:2′,3′-*b*′]bisporphyrinato}dipalladium(II) 8. 6″,6‴-{5,5′,10,10′,15,15′,20,20′-Octakis(3,5-di-*tert*-butylphenyl)quinoxalino[2,3-*b*:2′,3′-*b*′]bisporphyrin} **4** (100 mg, 0.0429 mmol) and palladium(II) chloride (70 mg, 0.395 mmol) were dissolved in toluene (15 cm^3) and glacial acetic acid (15 cm^3). The mixture was then heated at reflux for 72 h. The mixture was then diluted with chloroform (100 cm^3) and washed with water (2 × 100 cm^3), sodium carbonate solution (10%, 2 × 100 cm^3) then water (2 × 100 cm^3), dried over anhydrous sodium sulfate and filtered. The filtrate was evaporated to dryness and the residue purified by chromatography over silica (chloroform–light petroleum; 1 : 1). The major band was collected and the solvent removed to give *6″,6‴-{5,5′,10,10′,15,15′,20,20′-octakis(3,5-di-tert-butylphenyl)quinoxalino[2,3-b:2′,3′-b′]bisporphyrinato}dipalladium(II)* **8** (107 mg, 98%) as a red solid, mp > 300 °C (Found: C, 78.4; H, 8.05; N, 6.4. $C_{164}H_{186}N_{12}Pd_2$ + C_7H_8 (toluene) requires C, 78.1; H, 7.4; N, 6.4%). $\nu_{max}(CHCl_3)$/cm^{-1} 2964s, 2904m, 2868m, 1594s, 1477m, 1464w, 1427w, 1394w, 1364s, 1320w, 1300m and 1248m; $\lambda_{max}(CHCl_3)$/nm 356 (log ε 4.69), 407 (5.35), 446 (5.29), 466sh (5.22), 514 (4.39), 553 (4.73) and 590 (4.63); δ_H(400 MHz;

$CDCl_3$; Me_4Si) 1.49–1.57 (144 H, m, *t*-butyl H), 7.80–7.81 (4 H, m, aryl H), 7.96–7.99 (10 H, m, aryl H and biquinoxalinyl H-8), 8.01–8.03 (4 H, m, aryl H), 8.06 (8 H, t, *J* 1.8, aryl H), 8.16 (2 H, dd, *J* 1.9 and 8.8, biquinoxalinyl H-7), 8.19 (2 H, d, *J* 1.8, biquinoxalinyl H-5), 8.85 (4 H, br s, β-pyrrolic H), 8.86–8.89 (4 H, m, β-pyrrolic H), 8.960 (2 H, d, *J* 4.9, β-pyrrolic H) and 8.962 (2 H, d, *J* 4.9, β-pyrrolic H); *m*/*z* (MALDI-TOF) 2536 (M^+ requires 2535).

6″,6‴-{5,5′,10,10′,15,15′,20,20′-Octakis(3,5-di-*tert*-butylphenyl)quinoxalino[2,3-*b*:2′,3′-*b*′]bisporphyrinato}zinc(II) 9. 6″,6‴-{5,5′,10,10′,15,15′,20,20′-Octakis(3,5-di-*tert*-butylphenyl)-quinoxalino[2,3-*b*:2′,3′-*b*′]bisporphyrin} **4** (200 mg, 0.086 mmol) was dissolved in chloroform (25 cm^3) and heated at reflux with zinc(II) acetate dihydrate (19 mg, 0.088 mmol, 1 eq.) in methanol (1.5 cm^3) for 2 h. The reaction was followed by TLC (chloroform–light petroleum, 1 : 1). The solvent was removed and the residue was dissolved in chloroform (30 cm^3), washed with water (2 × 50 cm^3), dried over anhydrous sodium sulfate, filtered and the solvent removed. The product mixture was separated using flash chromatography (chloroform–light petroleum, 2 : 3). The first tan band eluted was evaporated to dryness and recrystallised to give free-base biquinoxalinyl bisporphyrin **4** (54 mg, 27%). The second brown band was treated in the same way and yielded *6″,6‴-{5,5′,10,10′,15,15′,20,20′-octakis(3,5-di-tert-butylphenyl)quinoxalino[2,3-b:2′,3′-b′]bisporphyrinato}zinc(II)* **9** (72 mg, 35%), mp > 300 °C (from chloroform and light petroleum). In a similar fashion, the last brown band was found to yield dizinc(II) biquinoxalinyl bisporphyrin **5** (42 mg, 20%). Analytically pure samples of the zinc(II) bis-porphyrin **9** were obtained by passing the compound through a short plug of silica, minimising exposure to light (Found: C, 82.1; H, 8.0; N, 7.1. $C_{164}H_{188}N_{12}Zn$ requires C, 82.3; H, 7.9; N, 7.0%); $\nu_{max}(CHCl_3)/cm^{-1}$ 3220, 2965, 2867, 1594, 1478, 1364, 1295, 1236 and 1151; $\lambda_{max}(CHCl_3)$/nm 415sh (log ε 5.40), 437 (5.50), 532 (4.52), 574 (4.42), 600 (4.30) and 618 (4.26); δ_H(400 MHz; $CDCl_3$; Me_4Si) −2.44 (2 H, s, inner NH), 1.51 (18 H, s, *t*-butyl H), 1.52 (18 H, s, *t*-butyl H), 1.54 (18 H, s, *t*-butyl H), 1.545 (18 H, s, *t*-butyl H), 1.547 (18 H, s, *t*-butyl H), 1.55 (18 H, s, *t*-butyl H), 1.57 (18 H, s, *t*-butyl H), 1.58 (18 H, s, *t*-butyl H), 7.80–7.82 (4 H, m, aryl H), 7.98–8.01 (2 H, m, aryl H and possible biquinoxalinyl H), 8.02–8.08 (12 H, m, aryl H and possible biquinoxalinyl H), 8.11–8.12 (8 H, m, aryl H), 8.13–8.19 (3 H, m, biquinoxalinyl H), 8.24 (1 H, d, $J_{5‴,7‴}$ 2.0 Hz, biquinoxalinyl H-5‴), 8.80 (2 H, s, H-12 and H-13 on FbP), 8.83 (2 H, s, H-12′ and H-13′ on ZnP), 9.01–9.04 (4 H, m, β-pyrrolic H on FbP) and 9.07–9.10 (4 H, m, β-pyrrolic H on ZnP); *m*/*z* (MALDI-TOF) 2392.5 (M^+ requires 2393).

Hexafluorophosphate[6″,6‴-{5,5′,10,10′,15,15′,20,20′-octakis-(3,5-di-*tert*-butylphenyl)quinoxalino[2,3-*b*:2′,3′-*b*′]bisporphyrinato}]aurate(III) 10. 6″,6‴-{5,5′,10,10′,15,15′,20,20′-Octakis-(3,5-di-*tert*-butylphenyl)quinoxalino[2,3-*b*:2′,3′-*b*′]bisporphyrin} **4** (240 mg, 0.103 mmol), potassium tetrachloroaurate(III) (100 mg, 0.265 mmol) and sodium acetate (80 mg, 0.975 mmol) were dissolved in a solution of chloroform (15 cm^3) and glacial acetic acid (18 M, 15 cm^3). The reaction mixture was then heated at reflux for 24 h. The solution was then allowed to cool and fresh potassium tetrachloroaurate(III) (100 mg, 0.264 mmol) and sodium acetate (90 mg, 1.097 mmol) were added with additional glacial acetic acid (18 M, 1 cm^3). The mixture was then heated at reflux for another 24 h, allowed to cool and further potassium tetrachloroaurate(III) (61 mg, 0.161 mmol), sodium acetate (59 mg, 0,72 mmol) and glacial acetic acid (18 M, 1 cm^3) were added. The mixture was heated at reflux for a further 24 h, allowed to cool and then diluted with chloroform (150 cm^3). The mixture was then washed with water (2 × 150 cm^3), sodium carbonate solution (10%, 2 × 150 cm^3), water (2 × 150 cm^3), dried over anhydrous sodium sulfate and filtered. The filtrate was evaporated to dryness and the residue dissolved in chloroform (15 cm^3). The organic phase was then stirred with a saturated solution of potassium hexafluorophosphate (1.86 g, 10.0 mmol) in water (10 cm^3) for 18 h. Chloroform (100 cm^3) was then added and the mixture washed with water (4 × 100 cm^3), dried over anhydrous sodium sulfate and filtered. The filtrate was evaporated to dryness and the residue purified by chromatography over silica (chloroform–methanol; 100 : 5). The first major band was collected and the solvent removed to give unreacted free-base biquinoxalinyl bisporphyrin **4** (50 mg). The second major band was collected and the solvent removed to give *hexafluorophosphate[6″,6‴-{5,5′,10,10′,15,15′,20,20′-octakis(3,5-di-tert-butylphenyl)quinoxalino-[2,3-b:2′,3′-b′]bisporphyrinato}]aurate(III)* **10** (157 mg, 60%) as a reddish-brown solid, mp > 300 °C; $\nu_{max}(CHCl_3)/cm^{-1}$ 3016s, 2962s, 2856m, 1726m, 1593m, 1466m, 1364m and 1248m; $\lambda_{max}(CH_2Cl_2)$/nm 424sh (log ε 5.22), 447 (5.42), 535 (4.49), 595 (4.32) and 654sh (3.50); δ_H(400 MHz; $CDCl_3$; Me_4Si) −2.49 (2 H, br s, inner NH), 1.40–1.50 (144 H, m, *t*-butyl H), 7.81–7.83 (2 H, m, H-7″ and H-5″ or H-8″), 7.91–7.93 (2 H, m, aryl H and biquinoxalinyl H), 8.01 (1 H, t, *J* 1.0, aryl H), 8.03 (2 H, d, *J* 1.6, aryl H), 8.04 (2 H, d, *J* 1.7, aryl H), 8.05–8.06 (3 H, m, aryl H), 8.07–8.08 (3 H, m, aryl H), 8.11–8.12 (6 H, m, aryl H), 8.13–8.14 (6 H, m, aryl H), 8.23 (1 H, d, *J* 2.0, H-5‴, H-8‴ or H-5″), 8.28 (1 H, d, *J* 2.0, H-5‴, H-8‴ or H-5″), 8.34 (1 H, dd, *J* 8.9 and 2.0, H-7‴), 8.80 (2 H, s, H-12 and H-13 on FbP), 9.04 and 9.13 (2 H, ABq, J_{AB} 4.6, β-pyrrolic H on FbP), 9.05 and 9.12 (2 H, ABq, J_{AB} 4.6, β-pyrrolic H on FbP), 9.24 (2 H, s, H-12′ and H-13′ on AuP), 9.25–9.28 (2 H, m, β-pyrrolic H on AuP), 9.35 (1 H, d, *J* 5.1, β-pyrrolic H on AuP) and 9.36 (1 H, d, *J* 5.1, β-pyrrolic H on AuP); δ_p(162 MHz; $CDCl_3$) −145.34 (1 P, h, *J* 713, PF_6); *m*/*z* (MALDI-TOF) 2524.5 ($[M\text{-}PF_6]^+$ requires 2524); *m*/*z* (FAB-MS) Found: $[M–PF_6]^+$ 2523.0. ($[M–PF_6]^+$ requires 2524).

Base line material from the column chromatography was collected and the solvent removed to give trace quantities of impure bis-chelated gold(III) 6″,6‴-{5,5′,10,10′,15,15′,20,20′-octakis(3,5-di-*tert*-butylphenyl)quinoxalino[2,3-*b*:2′,3′-*b*′]bisporphyrin} as a red-brown solid. *m*/*z* (MALDI-TOF) 2932, 2787, 2772, 2723, 1658 and 1590 ($[M\text{-}2PF_6]^+$ requires 2719).

Hexafluorophosphate[6″,6‴-{5,5′,10,10′,15,15′,20,20′-octakis(3,5-di-*tert*-butylphenyl)quinoxalino[2,3-*b*:2′,3′-*b*′]-bisporphyrinato}]zinc(II)aurate(III) 11. Hexafluorophosphate[6″,6‴-{5,5′,10,10′,15,15′,20,20′-octakis(3,5-di-*tert*-butylphenyl)-quinoxalino[2,3-*b*:2′,3′-*b*′]bisporphyrinato}]aurate(III) **10** (90 mg, 0.034 mmol) and zinc(II) acetate dihydrate (25 mg, 0.111 mmol) were dissolved in a solution of chloroform (14 cm^3) and methanol (1 cm^3). The mixture was then heated at reflux for 4 h. The mixture was then diluted with chloroform (100 cm^3) and washed with water (2 × 100 cm^3), dried over anhydrous sodium sulfate and filtered. The filtrate was evaporated to dryness and the residue dissolved in chloroform (15 cm^3). The organic phase was then stirred with a saturated solution of potassium hexafluorophosphate (2.79 g, 15.0 mmol) in water (15 cm^3) for 18 h. Chloroform (100 cm^3) was then added and the mixture was washed with water (4 × 100 cm^3), dried over anhydrous sodium sulfate and filtered. The solvent was removed under vacuum and the residue purified by chromatography over silica (chloroform–methanol; 100 : 6). The major polar band was collected, the solvent removed and the residue recrystallised from a chloroform–light petroleum solution (1 : 5) to afford hexafluorophosphate[6″,6‴-{5,5′,10,10′, 15,15′,20,20′-octakis(3,5-di-*tert*-butylphenyl)quinoxalino-[2,3-*b*:2′,3′-*b*′]bisporphyrinato}]zinc(II)aurate(III) **11** (80 mg, 87%) as green-blue crystals, mp > 300 °C; $\nu_{max}(CHCl_3)/cm^{-1}$ 3688w, 3606w, 2965s, 2868m, 1718w, 1593m, 1477m, 1427w, 1394w, 1364m, 1297w, 1248w, 1222s, 1214s and 1157w; $\lambda_{max}(CHCl_3)$/nm 354 (log ε 4.71), 392brsh (4.93), 421sh (5.27), 445 (5.42), 547 (4.46), 576 (4.47), 587brsh (4.42) and 615 (4.27);

δ_H(400 MHz; $CDCl_3$; Me_4Si) 1.53–1.59 (144 H, m, *t*-butyl H), 7.81–7.83 (2 H, m, aryl H), 7.92–7.94 (3 H, m, aryl H), 8.00–8.03 (4 H, m, aryl H and biquinoxalinyl H), 8.04–8.06 (6 H, m, aryl H and biquinoxalinyl H), 8.07–8.14 (11 H, m, aryl H and biquinoxalinyl H), 8.18 (1 H, dd, $J_{7'',8''}$ 8.8, $J_{7'',5''}$ 1.9, H-7″), 8.28–8.30 (2 H, m, biquinoxalinyl H), 8.36 (1 H, dd, $J_{7''',8'''}$ 8.9, $J_{7''',5'''}$ 1.9, H-7‴), 8.94 (2 H, s, H-12 and H-13 on ZnP), 9.04 and 9.08 (2 H, ABq, J_{AB} 4.6, β-pyrrolic H on ZnP), 9.05 and 9.09 (2 H, ABq, J_{AB} 4.6, β-pyrrolic H on ZnP), 9.25 (2 H, s, H-12′ and H-13′ on AuP), 9.26–9.27 (2 H, m, β-pyrrolic H on AuP), 9.35 (1 H, d, *J* 5.2, β-pyrrolic H on AuP) and 9.36 (1 H, d, *J* 5.1, β-pyrrolic H on AuP); δ_p(162 MHz; $CDCl_3$) −145.34 (1 P, h, *J* 713, PF_6); *m*/*z* (MALDI-TOF) 2588 ($[M–PF_6]^+$ requires 2588).

Synthesis of quinoxalino[2,3-*b*]porphyrins

5,10,15,20-Tetrakis(3,5-di-*tert*-butylphenyl)quinoxalino[2,3-*b*]-porphyrin 13. 2,3-Dioxo-5,10,15,20-tetrakis(3,5-di-*tert*-butylphenyl)chlorin **2** (246 mg, 0.225 mmol) and *o*-phenylenediamine **12** (120 mg, 1.10 mmol) were dissolved in dichloromethane (11 cm^3) and stirred for 6 h. The solvent was removed. The residue was dissolved in chloroform (50 cm^3), washed with water (2 × 100 cm^3), dried over anhydrous sodium sulfate and filtered. The solvent was removed and the residue was purified using flash chromatography (SiO_2, dichloromethane–light petroleum, 2 : 3). The front running major red band was collected and evaporated to dryness. This residue was recrystallised to afford red microcrystals of *5,10,15,20-tetrakis(3,5-di-tert-butylphenyl)quinoxalino[2,3-b]porphyrin* **13** (241 mg, 92%), mp > 300 °C (from dichloromethane and methanol) (Found: C, 84.7; H, 8.2; N, 7.3. $C_{82}H_{96}N_6$ requires C, 84.5; H, 8.3; N, 7.2%); $\nu_{max}(CHCl_3)/cm^{-1}$ 3350, 2967, 2905, 2869, 1593, 1478, 1364 and 1248; $\lambda_{max}(CHCl_3)$/nm 356 (log ε 4.36), 413sh (5.08), 434 (5.33), 493sh (3.70), 530 (4.27), 566 (3.84), 599 (4.03) and 651 (2.95); δ_H(400 MHz; $CDCl_3$; Me_4Si) −2.47 (2 H, s, inner NH), 1.49 (36 H, s, *t*-butyl H), 1.53 (36 H, s, *t*-butyl H), 7.72–7.75 (2 H, m, quinoxalino H), 7.80 (2 H, t, *J* 1.8, aryl H), 7.82–7.85 (2 H, m, quinoxalino H), 7.93 (2 H, t, *J* 1.8, aryl H), 7.98 (4 H, d, *J* 1.8, aryl H), 8.11 (4 H, d, *J* 1.8, aryl H), 8.80 (2 H, s, H-12 and H-13), 8.99 and 9.07 (4 H, ABq, J_{AB} 5.0, H-7, H-8, H-17 and H-18); *m*/*z* (MALDI-TOF) 1166 (M^+ requires 1166).

{5,10,15,20-Tetrakis(3,5-di-*tert*-butylphenyl)quinoxalino-[2,3-*b*]porphyrinato}zinc(II) 14. A solution of zinc(II) acetate dihydrate (220 mg, 1.0 mmol) in methanol (1 cm^3) was heated at reflux with 5,10,15,20-tetrakis(3,5-di-*tert*-butylphenyl)quinoxalino[2,3-*b*]porphyrin **13** (116 mg, 0.10 mmol) in dichloromethane (20 cm^3) for 30 min. The solution was evaporated to dryness, dissolved in dichloromethane (20 cm^3), washed with water (2 × 50 cm^3), dried over anhydrous sodium sulfate and filtered. The solvent was removed and the residue was purified using flash chromatography (SiO_2, dichloromethane–light petroleum, 2 : 3). The main red band was collected, evaporated to dryness and recrystallised to give *{5,10,15,20-tetrakis(3,5-di-tert-butylphenyl)quinoxalino[2,3-b]porphyrinato}zinc(II)* **14** (100 mg, 82%), mp > 300 °C (from dichloromethane and methanol) (Found: C, 78.95; H, 7.8; N, 6.95. $C_{82}H_{94}N_6Zn$ + H_2O requires C, 79.0; H, 7.8; N, 6.7%); $\nu_{max}(CHCl_3)/cm^{-1}$ 2959, 2932, 2906, 2869, 1593, 1478, 1462, 1394, 1364, 1342, 1298, 1174, 1135, 1118, 1015, 1007 and 938; $\lambda_{max}(CHCl_3)$/nm 337 (log ε 4.39), 412sh (5.10), 424 (5.11), 447 (5.09), 538 (3.80), 574 (4.20) and 618 (4.15); δ_H(400 MHz; $CDCl_3$; Me_4Si) 1.48 (36 H, s, *t*-butyl H), 1.53 (36 H, s, *t*-butyl H), 7.77–7.82 (2 H, m, quinoxalino H), 7.80 (2 H, t, *J* 1.8, aryl H), 7.88–7.92 (2 H, m, quinoxalino H), 7.93 (2 H, t, *J* 1.8, aryl H), 7.97 (4 H, d, *J* 1.8, aryl H), 8.10 (4 H, d, *J* 1.8, aryl H), 8.91 (2 H, s, H-12 and H-13), 9.00 and 9.05 (4 H, ABq, J_{AB} 5.0, H-7, H-8, H-17 and H-18); *m*/*z* (MALDI-TOF) 1229 (M^+ requires 1229).

{5,10,15,20-Tetrakis(3,5-di-*tert*-butylphenyl)quinoxalino-[2,3-*b*]porphyrinato}copper(II) 15. 5,10,15,20-Tetrakis(3,5-di-*tert*-butylphenyl)quinoxalino[2,3-*b*]porphyrin **13** (143 mg, 0.123 mmol) was dissolved in dichloromethane (30 cm^3) and a slurry of copper(II) acetate monohydrate (245 mg, 1.22 mmol) in methanol (25 cm^3) was added. The mixture was heated at reflux for 4 h and the solvent removed. The residue was dissolved in dichloromethane (50 cm^3), washed with water (2 × 100 cm^3), dried over anhydrous sodium sulfate, filtered and evaporated to dryness. The residue was recrystallised to afford brown microcrystals of *{5,10,15,20-tetrakis(3,5-di-tert-butylphenyl)quinoxalino[2,3-b]porphyrinato}copper(II)* **15** (134 mg, 89%), mp > 300 °C (from dichloromethane) (Found: C, 80.3; H, 7.7; N, 7.1. $C_{82}H_{94}N_6Cu$ requires C, 80.3; H, 7.7; N, 6.9%); $\nu_{max}(CHCl_3)/cm^{-1}$ 2967, 2906, 2869, 1594, 1478, 1466, 1426, 1394, 1364, 1347, 1300, 1248, 1181, 1120, 1010, 944, 899, 862 and 827; $\lambda_{max}(CHCl_3)$/nm 341 (log ε 4.41), 406 (5.11), 441 (5.10), 528 (3.89), 562 (4.19) and 606 (4.22); *m*/*z* (EI) 1226 (M^+, 100%).

{5,10,15,20-Tetrakis(3,5-di-*tert*-butylphenyl)quinoxalino-[2,3-*b*]porphyrinato}nickel(II) 16. 5,10,15,20-Tetrakis(3,5-di-*tert*-butylphenyl)quinoxalino[2,3-*b*]porphyrin **13** (157 mg, 0.135 mmol) was dissolved in dichloromethane (30 cm^3) and a solution of nickel(II) acetate tetrahydrate (160 mg, 1.36 mmol) in glacial acetic acid (15 cm^3) was added. The mixture was heated at reflux for 4 h, washed with water (2 × 100 cm^3), sodium carbonate solution (5%, 2 × 100 cm^3), water (2 × 100 cm^3), dried over anhydrous sodium sulfate, filtered and evaporated to dryness. The residue was recrystallised to afford brown microcrystals of *{5,10,15,20-tetrakis(3,5-di-tert-butylphenyl)quinoxalino[2,3-b]porphyrinato}nickel(II)* **16** (105 mg, 64%), mp > 300 °C (from dichloromethane and methanol) (Found: C, 80.5; H, 7.7; N, 7.1. $C_{82}H_{94}N_6Ni$ requires C, 80.6; H, 7.8; N, 6.9%); $\nu_{max}(CHCl_3)/cm^{-1}$ 2967, 2906, 2869, 1594, 1478, 1466, 1394, 1364, 1353, 1299 and 1248; $\lambda_{max}(CHCl_3)$/nm 339sh (log ε 4.39), 355 (4.45), 410 (5.01), 436 (5.09), 530 (4.03), 536sh (4.02), 560 (4.03) and 602 (4.09); δ_H(400 MHz; $CDCl_3$; Me_4Si) 1.42, 1.46 and 1.55 (72 H, s, *t*-butyl H), 7.70 (2 H, m, aryl H_p), 7.70 (4 H, d, *J* 1.8, aryl H), 7.72–7.76 (2 H, m, quinoxalino H), 7.75 (2 H, m, aryl H), 7.78–7.82 (2 H, m, quinoxalino H), 7.84 (4 H, d, *J* 1.8, aryl H), 8.68 (2 H, s, H-12 and H-13), 8.76 and 8.90 (4 H, ABq, J_{AB} 5, H-7, H-8, H-17 and H-18); *m*/*z* (EI) 1222 (M^+, 100%).

{5,10,15,20-Tetrakis(3,5-di-*tert*-butylphenyl)quinoxalino-[2,3-*b*]porphyrinato}palladium(II) 17. 5,10,15,20-Tetrakis(3,5-di-*tert*-butylphenyl)quinoxalino[2,3-*b*]porphyrin **13** (103 mg, 0.09 mmol) and palladium(II) chloride (91 mg, 0.513 mmol) were dissolved in toluene (20 cm^3) and glacial acetic acid (20 cm^3). The mixture was then heated at reflux for 48 h. The mixture was then diluted with dichloromethane (40 cm^3) and washed with water (100 cm^3), sodium carbonate solution (10%, 2 × 100 cm^3), water (2 × 100 cm^3), dried over anhydrous sodium sulfate and filtered. The filtrate was evaporated to dryness and the residue purified by chromatography over silica (dichloromethane–light petroleum; 1 : 3). The major band was collected and the solvent removed to give *{5,10,15,20-tetrakis(3,5-di-tert-butylphenyl)quinoxalino[2,3-b]porphyrinato}palladium(II)* **17** (98 mg, 88%) as a red solid, mp > 300 °C (from dichloromethane and methanol) (Found: C, 77.7; H, 7.5; N, 6.4. $C_{82}H_{94}N_6Pd$ requires C, 77.5; H, 7.5; N, 6.6%); $\nu_{max}(CHCl_3)/cm^{-1}$ 2964s, 2904m, 2869m, 1594s, 1477m, 1464w, 1427w, 1393w, 1364s, 1301w and 1248m; $\lambda_{max}(CHCl_3)$/nm 334sh (log ε 4.41), 345 (4.47), 401 (4.99), 436 (5.09), 510 (3.88), 545 (4.29) and 586 (4.37); δ_H(400 MHz; $CDCl_3$; Me_4Si) 1.48 (36 H, s, *t*-butyl H), 1.52 (36 H, s, *t*-butyl H), 7.75–7.80 (4 H, m, aryl H and quinoxaline H), 7.84–7.87 (2 H, m, quinoxaline H), 7.91–7.93 (6 H, m, aryl H), 8.05 (4 H, d, *J* 1.8, aryl H), 8.83 (2 H, s, H-12 and H-13), 8.84 and 8.92 (4 H, ABq, *J* 4.9, β-pyrrolic H); *m*/*z* (MALDI-TOF) 1271 (M^+ requires 1270).

Hexafluorophosphate{5,10,15,20-tetrakis(3,5-di-*tert*-butylphenyl)quinoxalino[2,3-*b*]porphyrinato}aurate(III) 18. 5,10,15,20-Tetrakis(3,5-di-*tert*-butylphenyl)quinoxalino[2,3-*b*]porphyrin **13** (100 mg, 0.086 mmol), potassium tetrachloroaurate(III) (80 mg, 0.211 mmol) and sodium acetate (70 mg, 1.30 mmol) were dissolved in a solution of chloroform (15 cm^3) and glacial acetic acid (18 M, 15 cm^3). The reaction mixture was then heated at reflux for 24 h. The mixture was then diluted with chloroform (100 cm^3) and washed with water (3 × 100 cm^3), sodium carbonate solution (10%, 2 × 100 cm^3), water (2 × 100 cm^3), dried over anhydrous sodium sulfate and filtered. The filtrate was removed under vacuum and the residue dissolved in chloroform (20 cm^3). The organic phase was then stirred with a saturated solution of potassium hexafluorophosphate (1.86 g, 10.1 mmol) in water (20 cm^3) for 24 h. The mixture was then diluted with chloroform (100 cm^3) and washed with water (4 × 100 cm^3), dried over anhydrous sodium sulfate and filtered. The filtrate was evaporated to dryness and the residue purified by chromatography over silica (chloroform–methanol; 100 : 5). The front running band was collected and the solvent removed to yield unreacted free-base quinoxalino[2,3-*b*]porphyrin **13** (25 mg).

The major polar band was collected and the solvent evaporated to dryness to afford *hexafluorophosphate{5,10,15,20-tetrakis(3,5-di-tert-butylphenyl)quinoxalino[2,3-b]porphyrinato}aurate(III)* **18** (60 mg, 51%) as a red-brown solid, mp > 300 °C; (FAB-HRMS found: $[M–PF_6]^+$ 1359.7206. $C_{82}H_{94}N_6Au$ requires 1359.7212); $\nu_{max}(CHCl_3)/cm^{-1}$ 3688w, 3018w, 2965s, 2870m, 1734s, 1594m, 1477w, 1395m, 1365w, 1300m, 1247m, 1214m, 1124w, 1064w and 1032w; $\lambda_{max}(CHCl_3)$/nm 344 (log ε 4.37), 392 (4.58), 418brsh (4.83), 436 (5.28), 510sh (3.88), 545 (4.05) and 587 (4.10); δ_H(400 MHz; $CDCl_3$) 1.48 (36 H, s, *t*-butyl H), 1.53 (36 H, s, *t*-butyl H), 7.91 (2 H, t, *J* 1.6, aryl H), 7.93 (4 H, d, *J* 1.6, aryl H), 7.94–7.98 (4 H, m, quinoxalino H), 8.01 (2 H, t, *J* 1.6, aryl H), 8.07 (4 H, d, *J* 1.6, aryl H), 9.23 (2 H, s, H-12 and H-13), 9.24 and 9.33 (4 H, ABq, J_{AB} 5.1, H-7, H-8, H-17 and H-18); δ_P(162 MHz; $CDCl_3$) −145.34 (1 P, h, *J* 713, PF_6); *m*/*z* (MALDI-TOF) 1360.5 ($[M–PF_6]^+$ requires 1361).

Acknowledgements

We thank the Australian Research Council for research grants to M. J. C. and the Australian Post-graduate Research Award to R. W. and P. J. S.

References

1 J. Deisenhofer, O. Epp, K. Miki, R. Huber and H. Michel, *Nature (London)*, 1985, **318**, 618–623.
2 R. F. Franzen, R. A. Goldstein and S. G. Boxer, *J. Phys. Chem.*, 1993, **97**, 3040–3053.
3 J. Deisenhofer and H. Michel, *Science*, 1989, **245**, 1463–1473.
4 P. Jordan, P. Fromme, H. T. Witt, O. Klukas, W. Saenger and N. Krauss, *Nature (London)*, 2001, **411**, 909–917.
5 A. Zouni, H. T. Witt, J. Kern, P. Fromme, N. Krauss, W. Saenger and P. Orth, *Nature (London)*, 2001, **409**, 739–743.
6 V. S.-Y. Lin, S. G. Dimango and M. J. Therien, *Science*, 1994, **264**, 1105–1111.
7 H. L. Anderson, *Inorg. Chem.*, 1994, **33**, 972–981.
8 K. A. Jolliffe, T. D. M. Bell, K. P. Ghiggino, S. J. Langford and M. N. Paddon-Row, *Angew. Chem., Int. Ed.*, 1998, **37**, 916–919.
9 J. Li, J. R. Diers, J. Seth, S. I. Yang, D. F. Bocian, D. Holten and J. S. Lindsey, *J. Org. Chem.*, 1999, **64**, 9090–9100.
10 J. L. Sessler, B. Wang, S. L. Springs and C. T. Brown, in *Comprehensive Supramolecular Chemistry*, ed. J. L. Atwood, J. E. D. Davies, D. D. MacNicol and F. Vögtle, Elsevier Science Ltd, Oxford, 1996, vol. 4, pp. 311–336.
11 R. A. Haycock, A. Yartsev, U. Michelsen, V. Sundström and C. A. Hunter, *Angew. Chem., Int. Ed.*, 2000, **39**, 3616–3619.
12 J.-C. Chambron, V. Heitz and J.-P. Sauvage, in *The Porphyrin Handbook*, ed. K. M. Kadish, K. M. Smith and R. Guilard, Academic Press, San Diego, CA, 2000, vol. 6, pp. 1–42.
13 A. Tsuda, H. Furuta and A. Osuka, *J. Am. Chem. Soc.*, 2001, **123**, 10304–10321.
14 N. Aratani, A. Osuka, H. S. Cho and D. Kim, *J. Photochem. Photobiol. C*, 2002, **3**, 25–52.
15 T. X. Lü, J. R. Reimers, M. J. Crossley and N. S. Hush, *J. Phys. Chem.*, 1994, **98**, 11878–11884.
16 HYPERCHEM version 6.01, Hypercube Inc, Gainesville, FL, 2000.
17 M. J. Crossley, A. C. Try and R. Walton, *Tetrahedron Lett.*, 1996, **37**, 6807–6810.
18 E. K. L. Yeow, P. J. Sintic, N. M. Cabral, J. N. H. Reek, M. J. Crossley and K. P. Ghiggino, *Phys. Chem. Chem. Phys.*, 2000, **2**, 4281–4291.
19 M. J. Crossley and P. L. Burn, *J. Chem. Soc., Chem. Commun.*, 1987, 39–40.
20 M. J. Crossley and P. L. Burn, *J. Chem. Soc., Chem. Commun.*, 1991, 1569–1571.
21 M. J. Crossley, L. J. Govenlock and J. K. Prashar, *J. Chem. Soc., Chem. Commun.*, 1995, 2379–2380.
22 W. A. Hough, PhD Thesis, The University of Sydney, 2003.
23 S. Fukuzumi, M. J. Crossley and P. J. Sintic, unpublished results.
24 A. D. Becke, *J. Chem. Phys.*, 1993, **98**, 5648–5652.
25 J. S. Binkley, J. A. Pople and W. J. Hehre, *J. Am. Chem. Soc.*, 1980, **102**, 939–947.
26 M. J. Frisch, G. W. Trucks, H. B. Schlegel, G. E. Scuseria, M. A. Robb, J. R. Cheeseman, V. G. Zakrzewski, J. A. Montgomery, Jr., R. E. Stratmann, J. C. Burant, S. Dapprich, J. M. Millam, A. D. Daniels, K. N. Kudin, M. C. Strain, O. Farkas, J. Tomasi, V. Barone, M. Cossi, R. Cammi, B. Mennucci, C. Pomelli, C. Adamo, S. Clifford, J. Ochterski, G. A. Petersson, P. Y. Ayala, Q. Cui, K. Morokuma, D. K. Malick, A. D. Rabuck, K. Raghavachari, J. B. Foresman, J. Cioslowski, J. V. Ortiz, B. B. Stefanov, G. Liu, A. Liashenko, P. Piskorz, I. Komaromi, R. Gomperts, R. L. Martin, D. J. Fox, T. Keith, M. A. Al-Laham, C. Y. Peng, A. Nanayakkara, C. Gonzalez, M. Challacombe, P. M. W. Gill, B. G. Johnson, W. Chen, M. W. Wong, J. L. Andres, M. Head-Gordon, E. S. Replogle and J. A. Pople, GAUSSIAN 98 (Revision A.7), Gaussian, Inc., Pittsburgh, PA, 1998.
27 J. Zeng, N. S. Hush and J. R. Reimers, *J. Am. Chem. Soc.*, 1996, **118**, 2059–2068.
28 J. E. Ridley and M. C. Zerner, *Theor. Chim. Acta*, 1973, **32**, 111–134.
29 M. Maruyama and K. Murakami, *J. Electroanal. Chem.*, 1979, **102**, 221–235.
30 A. Ghosh, I. Halvorsen, H. J. Nilsen, E. Steene, T. Wondimagegn, R. Lie, E. van Caemelbecke, N. Guo, Z. Ou and K. M. Kadish, *J. Phys. Chem. B*, 2001, **105**, 8120–8124.
31 K. M. Kadish, M. Lin, E. Van Caemelbecke, G. De Stefano, C. J. Medforth, D. J. Nurco, N. Y. Nelson, B. Krattinger, C. M. Muzzi, L. Jaquinod, Y. Xu, D. C. Shyr, K. M. Smith and J. A. Shelnutt, *Inorg. Chem.*, 2002, **41**, 6673–6687.
32 K. M. Kadish, W. E, Z. Ou, J. Shao, P. J. Sintic, K. Ohkubo, S. Fukuzumi and M. J. Crossley, *Chem. Commun.*, 2002, 356–357.
33 M. J. Crossley, P. J. Sintic, R. Walton, W. E, Z. Ou, J. Shao and K. M. Kadish, unpublished results.
34 M. Kasha, H. R. Rawls and M. A. El-Bayoumi, *Pure Appl. Chem.*, 1965, **11**, 371–392.
35 K. Sendt, L. A. Johnston, W. A. Hough, M. J. Crossley, N. S. Hush and J. R. Reimers, *J. Am. Chem. Soc.*, 2002, **124**, 9299–9309.